Research Article | Vol. 6, No. 9 | 1 Sep 2016 | OPTICAL MATERIALS EXPRESS 2834

Optical Materials EXPRESS

Color-tunable stacked organic light-emitting diode with semi-transparent metal electrode

SEOK-HWAN CHUNG* AND HEE YEON NOH

Nano-Energy Convergence Research Division, Daegu Gyeongbuk Institute of Science and Technology (DGIST), 333 Techno Jungang-daero, Hyeonpung-myeon, Dalseong-gun, Daegu 42988, South Korea
chungsh@dgist.ac.kr

Abstract: Stacked organic light-emitting diode (OLED) devices with two terminals have been fabricated by successive application of solution coating and vacuum deposition. We seamlessly engineered the two processing steps by optimizing the semi-transparent metal electrode and the carrier transport buffer layer, and investigated the electrical and optical properties of the thus-prepared devices. The top and bottom OLEDs can be independently addressed by switching the polarity of the voltage applied to the two terminals. The emission color from the stacked OLED devices is easily tuned between green and blue or red and blue, by adjusting the offset of the alternating current applied to the stacked OLED devices. Thus, a simple approach is presented towards printable and color-tunable organic lighting for the future.

OCIS codes: (230.2090) Electro-optical devices; (230.3670) Light-emitting diodes; (120.2040) Displays; (160.4890) Organic materials; (310.6845) Thin film devices and applications.

References and links

1. S. Reineke, F. Lindner, G. Schwartz, N. Seidler, K. Walzer, B. Lüssem, and K. Leo, "White organic light-emitting diodes with fluorescent tube efficiency," Nature **459**(7244), 234–238 (2009).
2. E. L. Williams, K. Haavisto, J. Li, and G. E. Jabbour, "Excimer-based white phosphorescent organic light emitting diodes with nearly 100% internal quantum efficiency," Adv. Mater. **19**(2), 197–202 (2007).
3. I. A. Barlow, T. Kreouzis, and D. G. Lidzey, "High-speed electroluminescence modulation of a conjugated-polymer light emitting diode," Appl. Phys. Lett. **94**(24), 243301 (2009).
4. C. D. Müller, A. Falcou, N. Reckefuss, M. Rojahn, V. Wiederhirn, P. Rudati, H. Frohne, O. Nuyken, H. Becker, and K. Meerholz, "Multi-colour organic light-emitting displays by solution processing," Nature **421**(6925), 829–833 (2003).
5. C. Chu, J. Ha, J. Choi, S. Lee, J. Rhee, D. Lee, J. Chung, H. Kim, and K. Chung, "Advances and issues in white OLED and color filter architecture," SID 07 Digest, **38**(1), 1118–1121 (2007).
6. J. Kido, M. Kimura, and K. Nagai, "Multilayer white light-emitting organic electroluminescent device," Science **267**(5202), 1332–1334 (1995).
7. L. S. Liao, K. P. Klubek, and C. W. Tang, "High efficiency tandem organic light-emitting diodes," Appl. Phys. Lett. **84**(2), 167 (2004).
8. G.-K. Ho, H.-F. Meng, S.-C. Lin, S.-F. Horng, C.-S. Hsu, L.-C. Chen, and S.-M. Chang, "Efficient white light emission in conjugated polymer homojunctions," Appl. Phys. Lett. **85**(20), 4576 (2004).
9. Q. J. Sun, J. H. Hou, C. H. Yang, Y. F. Li, and Y. Yang, "Enhanced performance of white polymer light-emitting diodes using polymer blends as hole-transporting layers," Appl. Phys. Lett. **89**(15), 153501 (2006).
10. Z. Shen, P. E. Burrows, V. Bulovic, S. R. Forrest, and M. E. Thompson, "Three-color, tunable, organic light-emitting devices," Science **276**(5321), 2009–2011 (1997).
11. P. E. Burrows, G. Gu, S. R. Forrest, E. P. Vicenzi, and T. X. Zhou, "Semitransparent cathodes for organic light emitting devices," J. Appl. Phys. **87**(6), 3080 (2000).
12. S. Han, X. Feng, Z. H. Lu, D. Johnson, and R. Wood, "Transparent-cathode for top-emission organic light-emitting diodes," Appl. Phys. Lett. **82**(16), 2715 (2003).
13. G. Gu, V. Khalfin, and S. R. Forrest, "High-efficiency, low-drive-voltage, semitransparent stacked organic light-emitting device," Appl. Phys. Lett. **73**(17), 2399 (1998).
14. H. Peng, J. Sun, X. Zhu, X. Yu, M. Wong, and H.-S. Kwok, "High-efficiency microcavity top-emitting organic light-emitting diodes using silver anode," Appl. Phys. Lett. **88**(7), 073517 (2006).
15. C. J. Liang and W. C. H. Choy, "Tunable full-color emission of two-unit stacked organic light emitting diodes with dual-metal intermediate electrode," J. Organomet. Chem. **694**(17), 2712–2716 (2009).
16. T. Matsushima, Y. Kinoshita, and H. Murata, "Formation of Ohmic hole injection by inserting an ultrathin layer of molybdenum trioxide between indium tin oxide and organic hole-transporting layers," Appl. Phys. Lett. **91**(25), 253504 (2007).

#266579 http://dx.doi.org/10.1364/OME.6.002834
Journal © 2016 Received 25 May 2016; revised 28 Jul 2016; accepted 28 Jul 2016; published 10 Aug 2016

Optical Materials EXPRESS

17. Q. Y. Bao, J. P. Yang, Y. Q. Li, and J. X. Tang, "Electronic structures of MoO_3-based charge generation layer for tandem organic light-emitting diodes," Appl. Phys. Lett. **97**(6), 063303 (2010).
18. C.-W. Chu, S.-H. Li, C.-W. Chen, V. Shrotriya, and Y. Yang, "High-performance organic thin-film transistors with metal oxide/metal bilayer electrode," Appl. Phys. Lett. **87**(19), 193508 (2005).
19. C. W. Ko and Y. T. Tao, "Bright white organic light-emitting diode," Appl. Phys. Lett. **79**(25), 4234 (2001).
20. Y. S. Lee, J.-H. Park, and J. S. Choi, "Frequency-dependent electrical properties of organic light-emitting diodes," J. Korean Phys. Soc. **42**, 294 (2003).
21. V. Bulovic, V. B. Kahlfin, G. Gu, P. E. Burrows, D. Z. Garbuzov, and S. R. Forrest, "Weak microcavity effects in organic light-emitting devices," Phys. Rev. B **58**(7), 3730–3740 (1998).

1. Introduction

Lighting technology based on organic materials has been drawing tremendous attention of late, due to its potential in substituting established technologies like incandescent lighting, fluorescent lighting, and solid-state light-emitting diodes (LED). Organic LED (OLED) lighting technology based on organic emissive materials already demonstrates very high energy efficiency compared to that of white fluorescent tube and internal quantum efficiency (IQE) of ~100% [1,2]. The emission control is also faster than that of the liquid-crystal-based technology [3]. OLED lighting is considered an environment-friendly lighting technology because it does not require toxic elements like mercury and it does not emit ultraviolet radiation. Furthermore, it presents the advantage of conformal, flexible, printable, and homogeneous two-dimensional (2D) surface lighting.

Unlike conventional lighting technologies, OLED lighting offers the additional advantage of facile tuning of the emission colors of the homogenous 2D surface. The color-tuning methods for OLED devices include controlled light emission from parallel red-green-blue (RGB) elements [4], micro-patterned color filters in conjunction with white OLED backlight [5], RGB multilayer stacking [6,7], and a single polymer emission layer by controlled doping or blending [8,9]. However, these methods either do not allow electrical control of emission colors [1,6] or require additional multi-step lithographic processes [4,10].

In this study, we demonstrate a color-tunable lighting concept, using a stacked OLED structure with two terminals. The device was fabricated with successive application of solution coating and vacuum deposition processes, for each organic light emission structure. The intermediate semi-transparent metal electrode allows high optical transmission as well as high conductivity. The thermal evaporation of the metal electrode causes less damage to the organic materials compared to the radio-frequency sputtering of the transparent oxide electrode [11,12]. Depending on the offset of the AC voltage, the emission colors can be controlled between green and blue or red and blue. Unlike other color-tuning methods, the usage of an AC voltage is readily compatible with household power supplies and also, it allows a simultaneous control of the colors from the top and the bottom emission layers.

2. Experimental

Figure 1 shows (a) the schematic illustration of the stacked OLED device, and (b) the molecular structures of the organic materials used in this work. The stacked OLED structure is composed of a top OLED, an intermediate contact, and a bottom OLED. The top electrode is directly connected to the bottom electrode as shown in Fig. 1(a). A DC or AC voltage is applied between the top-bottom electrode and the intermediate electrode. The top and the bottom OLEDs emit different colors depending on the current polarity. The bottom structure was fabricated by a spin-coating process using the polymer solution while the top structure, was fabricated via the conventional vacuum deposition process. The indium tin oxide (ITO) bottom electrode on the glass substrate was 150nm thick and its sheet resistance was about 12Ω/sq. Firstly, the bottom ITO electrode was cleaned by subsequent ultrasonic treatments in acetone, methanol, and deionized water. Thereafter, a hole injection layer poly(ethylenedioxythiophene):polystyrenesulphonate (PEDOT:PSS) was spin-coated at 3000rpm for 60s after purification. The PEDOT:PSS (30nm) was then baked at 110°C for 15min. The polymers N,N'-diphenyl-N,N'-bis-(3-methylphenyl)-[1,1'-biphenyl]-4,4'-diamine

Optical Materials EXPRESS

(poly-TPD) blended with poly(9-vinylcarbazole) (PVK) dissolved in toluene (1wt%) and poly[9,9-dioctylfluorenyl-2,7-diyl] (PFO) end capped with dimethylphenyl (DMP) in toluene (1wt%) were utilized for the hole transport and the blue emission layer, respectively. Both solutions were spin-coated at 4000rpm for 60s. The poly-TPD:PVK (30nm) and the PFO (60nm) layers were then baked at 120°C for 20min and for 30min, respectively. The solution coating of the OLED devices was conducted at room temperature under ambient condition.

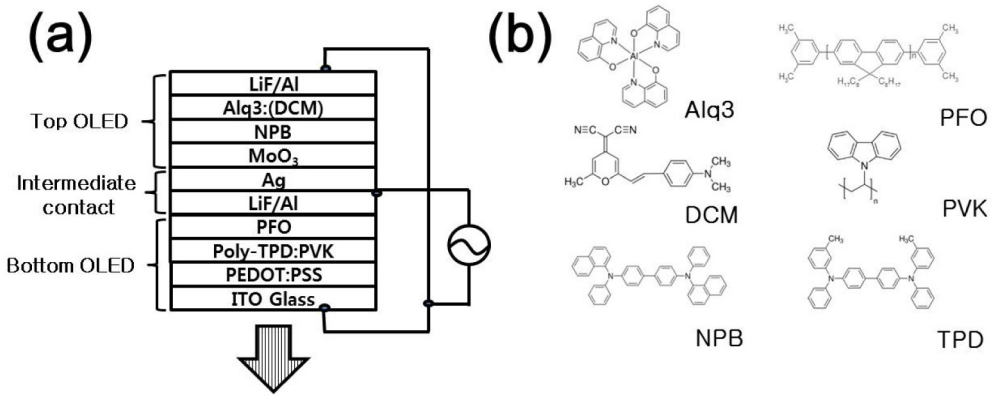

Fig. 1. (a) Schematic illustration of the color tunable OLED device, and (b) molecular structure of organic materials used in the OLED device.

The intermediate contact and the top structure were fabricated by thermal deposition under high vacuum right after the solution coating of the bottom structure. The intermediate contact was a dual metal structure composed of Al (3nm) and Ag (15nm). The deposition rate was 1.5Å/s for Al and 2.0Å/s for Ag. The contact was optimized for low resistance and high transmittance and selected to minimize the degradation of bottom organic layers. The sheet resistance was about 3.7Ω/sq., and the optical transmittance was approximately 44%. Molybdenum trioxide (MoO_3) was then thermally evaporated for effective hole injection to the top OLED. For the top emission structure, N,N'-diphenyl-N,N'-bis-(3-methylphenyl)-[1,1'-biphenyl]-4,4'-diamine (NPB) (50nm) and tris-(8-hydroxyquinoline)-aluminum (Alq3) (50nm) were used as the hole transport layer and the green emission layer, respectively. For red emission, 10% of 4-(dicyanomethylene)-2-methyl-6-(4-dimethylaminostyryl)-4H-pyran (DCM) was doped in Alq3 by co-deposition from two separate sources. The deposition of small organic molecules was done by slow heating up to their sublimation temperatures at a background pressure of 2×10^{-6} Torr. The deposition rate was 0.1-1Å/s. The top electrode was composed of LiF (1nm) and Al (100nm) layers, which were also deposited by thermal evaporation under high vacuum. The deposition rate was 0.1Å/s for LiF and 3-4Å/s for Al. The active emission area was 3×3 mm^2.

The whole stacked OLED structure was ITO/PEDOT:PSS/Poly-TPD:PVK/PFO/LiF/Al/Ag/MoO_3/NPB/Alq3/LiF/Al for the green to blue tuning OLED (GB-OLED). As for the red to blue tuning OLED (RB-OLED), Alq3:DCM was used instead of Alq3. The characterization of the OLED devices was conducted at room temperature, under ambient conditions, without light out-coupling and device encapsulation. Current-voltage characteristics of the OLED devices were measured by a source-meter (Keithley 2450) while a DC current was applied between the two terminals of the OLED devices. The luminance, emission spectrum, and the Commission internationale de l'éclairage (CIE) coordinates were measured by a spectrometer (Minolta, CS-1000). For the application of an AC current with variable waveform, a function generator and a high-voltage amplifier were used.

Optical Materials EXPRESS

3. Results and discussion

Initially, we examined the intermediate electrode structure that is important for the connection of the top and the bottom OLEDs as well as for the operation of the stacked OLED devices. Since the intermediate electrode is used as a cathode for the bottom OLED and as an anode for the top OLED, it should efficiently provide both electron injection and hole injection [13–15]. In addition to the high conductance required for an electrode, it is required to also offer proper optical transparency, because the light from the top OLED has to pass through the intermediate electrode. In this work, an Al/Ag dual-metal electrode was used because Al is known to be a good cathode material and Ag has a good optical transmittance [14]. Figure 2(a) shows the emission property of the bottom OLED structure (ITO/PEDOT:PSS/Poly-TPD:PVK/PFO/LiF/Al/Ag) with different thicknesses of Al. As the thickness of Al increases, the turn-on voltage decreases and the device shows an enhanced luminance mainly as a result of an improved electron injection and less emission loss. The optical transparency of the 5nm Al electrode was however poor. Hence, the Al (3nm)/Ag (15nm) bilayer was selected as the intermediate electrode for this work.

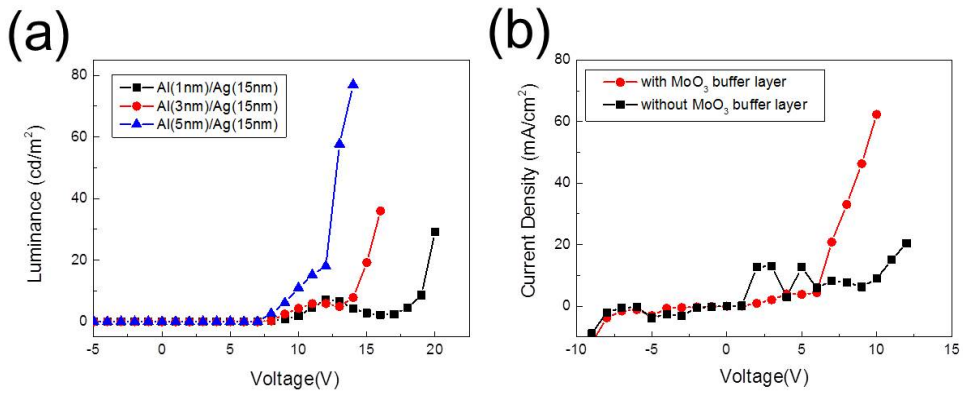

Fig. 2. (a) Luminance vs. applied voltage for the blue emitting polymer OLED with different top electrodes. (b) Current density vs. applied voltage for the GB-OLED device, with and without the MoO_3 buffer layer.

Figure 2(b) shows the current-voltage characteristics of the stacked OLED, with and without the oxide buffer layer. In general, Ag is a well-known anode material for OLED devices [1,6,10]. However, it is not a good cathode material since it has a low work function (~4.2eV). In order to enhance hole injection in this work, a transition metal oxide MoO_3 is used as a buffer layer between Ag and NPB [16,17]. The hole injection buffer layer substantially reduces the threshold voltage because it lowers the injection barrier and minimizes chemical reactivity between the metallic electrode and the hole transport organic layer [18].

Figures 3(a) and 3(b) show the electro-optical properties of the color-tunable stacked OLED devices. When a DC voltage of negative polarity is applied between the two terminals, green (λ_p = ~530nm) or red (λ_p = ~600nm) light is emitted from the top emissive layer. Red emission from the Alq3:DCM is mainly due to direct recombination at the dopant sites [19]. However, when a DC voltage with positive polarity is applied to the two terminals, blue (λ_p = ~435nm and ~460nm) light is emitted from the bottom PFO emissive layer. Figure 3(a) shows the current density as a function of the applied DC voltage to the stacked OLED device. The current density begins to increase at −7V for negative polarity and at 8V, for positive polarity for the GB-OLED device. Note that there are kinks near ± 4V. These may be associated with a transition from an ohmic current to a space-charge-limited current [20]. Luminance from the device also begins to increase at −7V and 8V as shown in Fig. 3(b). The green emission is

Optical Materials EXPRESS

about 134cd/m^2 at −10V, and the blue emission is roughly 42cd/m^2 at 13V. The power efficiency for the top and the bottom OLED devices are ~0.1 lm/W at −10V and ~0.05 lm/W at 10V, respectively. For red emission of the RB-OLED device, the turn-on voltage is about −9V,and the luminance is approximately 62cd/m^2 at −15V. The current density and the luminance for positive polarity corresponding to blue emission of the RB-OLED device are almost identical to that of the GB-OLED device. The luminance of the top layer is slightly higher than that of the bottom layer, even though the light passes through the intermediate dual-metal contact and the bottom organic materials. An estimated energy level diagram of the stacked OLED device is provided in Fig. 3(c).

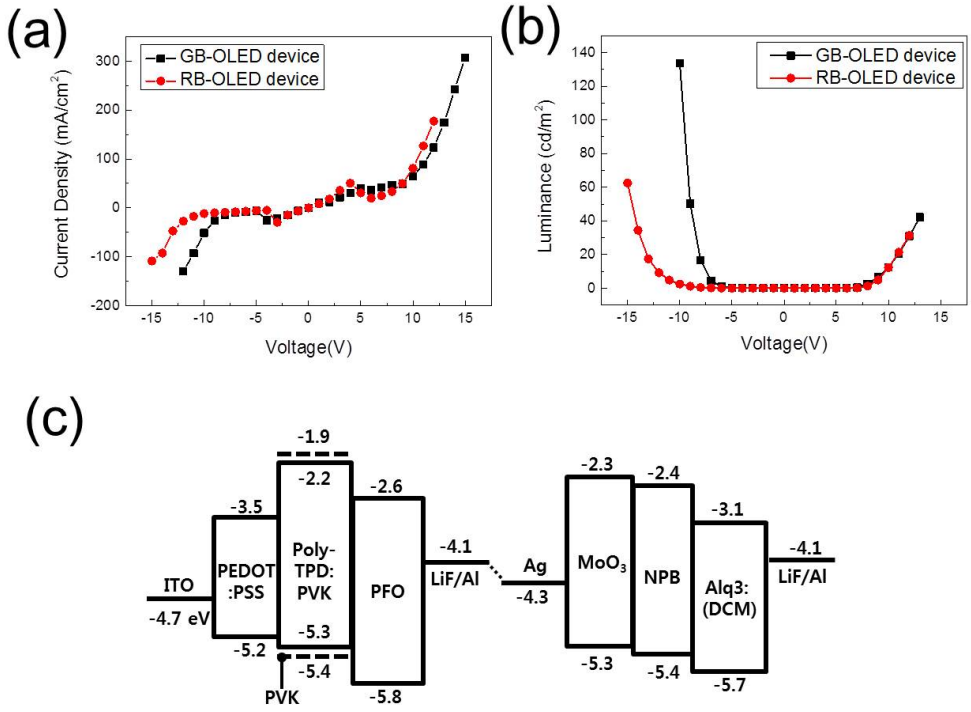

Fig. 3. (a) Current density vs. applied voltage, and (b) luminance vs. applied voltage for GB- and RB-OLED devices. (c) Estimated energy level diagram of the OLED device showing the work function, HOMO and LUMO level of the respective layers.

Figure 4 shows the change of the spectrum as a function of the applied DC voltage for (a) GB-OLED and (b) RB-OLED devices. The figures clearly demonstrate the dependence of the emission spectrum on applied voltages. For negative polarity, the spectrum shows single green (λ_p = ~530nm) or red peak (λ_p = ~600nm) from the top OLED. The intensity then diminishes as the current density decreases. When the polarity of the applied voltage is reversed, the blue emission spectrum with multi-peaks from the bottom OLED emerges. The spectrum shape and the emission peak positions do not alter as the intensity changes with applied voltage. Compared to the broad red spectrum in the RB-OLED device, the green spectrum in the GB-OLED device is narrow. This is associated with a weak microcavity effect of the top OLED of the GB-OLED device [21]. The corresponding changes of the CIE coordinates are from (0.26, 0.64) to (0.19, 0.17) for the GB-OLED device and from (0.58, 0.42) to (0.19, 0.17) for the RB-OLED device, respectively.

Optical Materials EXPRESS

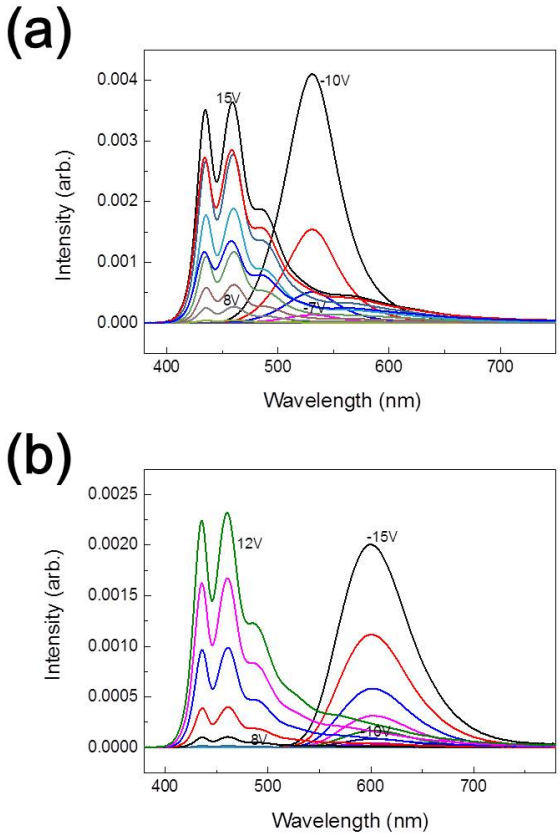

Fig. 4. Emission spectrum at different applied DC voltages (ΔV = 1V) for (a) GB-OLED, and (b) RB-OLED devices.

To demonstrate the ability of color-tuning, sinusoidal AC voltages (1kHz, $10V_{pp}$) with different offset values were applied to the two terminals of the OLED devices. As shown in Figure 5, the color coordinate of the GB-OLED device changes from (0.25, 0.61) to (0.19, 0.17) as the offset varies from −1.00V to 1.50V (ΔV = 0.25V). The color coordinate of the RB-OLED device changes from (0.57, 0.40) to (0.19, 0.15) as the offset varies from −1.25V to 0V (ΔV = 0.25V) and 1.00V. The alteration of the color coordinate occurs along a straight line. The offset voltage tunes the colors by controlling the relative amount of different color photons emitted from the top and the bottom OLED devices. In addition to this, the coordinate change is not a fixed step. This is not only due to the sinusoidal waveform but also, due to the asymmetric turn-on voltage and unsymmetrical luminance of the top and the bottom OLEDs as shown in Fig. 3(b). Nonetheless, this result clearly demonstrates that the color of the stacked OLED devices can be easily tuned by adjusting the relative amount of emission from the top and the bottom OLEDs using only the offset voltage.

Optical Materials EXPRESS

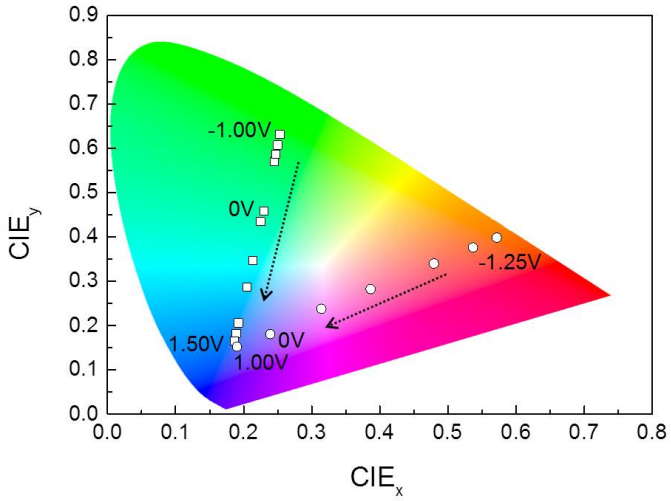

Fig. 5. CIE coordinates as a function of the offset of applied sinusoidal AC voltages (1kHz, $10V_{pp}$) for (a) GB-OLED and (b) RB-OLED devices. The color of the GB-OLED device changes from (0.25, 0.61) to (0.19, 0.17) as offset varies from −1.00V to 1.50V (ΔV = 0.25V). The color of the RB-OLED device changes from (0.57, 0.40) to (0.19, 0.15) as offset varies from −1.25V to 0V (ΔV = 0.25V) and 1.00V.

4. Conclusion

In summary, we have fabricated color-tunable stacked OLED devices and investigated their electrical and optical properties. This work has demonstrated a simple color-tuning method in stacked OLED lighting devices fabricated by subsequent solution coating and vacuum deposition processes. We optimized and seamlessly connected the two processing steps by carefully engineering the semi-transparent metal electrode and the carrier transport buffer layers. The emission colors can easily be tuned by electrically addressing the top and the bottom OLEDs with an AC voltage, which is conveniently compatible with a conventional household power supply. Future work will include lowering the turn-on voltage, enhancing the light out-coupling and engineering the CIE coordinates for tuning colors through white emission.

Acknowledgment

This work was supported by the DGIST R&D Program of the Ministry of Science, ICT & Future Planning of Korea [16-NB-05].